Separation Science and Technology
Publication details, including instructions for authors and subscription information:
http://www.informaworld.com/smpp/title~content=t713708471

Rolltruded Poly(Aryl Ether Ether Ketone) (PEEK) for Membrane Applications

R. J. Ciora JR.[a]; J. H. Magill[a]
[a] DEPARTMENT OF CHEMICAL AND PETROLEUM ENGINEERING, UNIVERSITY OF PITTSBURGH PITTSBURGH, PENNSYLVANIA, USA

To cite this Article Ciora JR., R. J. and Magill, J. H.(1997) 'Rolltruded Poly(Aryl Ether Ether Ketone) (PEEK) for Membrane Applications', Separation Science and Technology, 32: 5, 899 — 923
To link to this Article: DOI: 10.1080/01496399708000935
URL: http://dx.doi.org/10.1080/01496399708000935

SEPARATION SCIENCE AND TECHNOLOGY, **32**(5), pp. 899–923, 1997

Rolltruded Poly(Aryl Ether Ether Ketone) (PEEK) for Membrane Applications

R. J. CIORA , JR. and J. H. MAGILL*
DEPARTMENT OF CHEMICAL AND PETROLEUM ENGINEERING
UNIVERSITY OF PITTSBURGH
PITTSBURGH, PENNSYLVANIA 15261, USA

ABSTRACT

An investigation of the transport and separation of several permanent gases (CO_2, N_2, CH_4, and H_2) and vapors (H_2O and ethanol) in unprocessed and rolltruded poly(aryl ether ether ketone) (PEEK) thin films has been conducted to evaluate PEEK for membrane applications requiring thermally and chemically stable materials. Transport coefficients and separation factors have been determined at permeation temperatures ranging from 40 to ca. 180°C. The gas transport coefficients were found to increase by up to 30% depending on the processing conditions. Actual separation factors, determined for a CO_2/N_2 gas mixture (24.6 vol% CO_2), were depressed slightly in comparison to the ideal values obtained from pure component data. In contrast, water and ethanol vapor permeabilities declined between 10 and 15% as a result of processing. For a 39.1 wt% vapor mixture of H_2O in EtOH, ideal and actual separation factors, determined at 130°C, were in good agreement. In contrast, order of magnitude improvements in the actual versus ideal separation factors were found for 11.7 and 7.6 wt% mixtures of H_2O in EtOH in both unprocessed and rolltruded PEEK. A comparison with other membranes considered for high temperature vapor dehydrations suggests that PEEK may be an excellent polymer for these applications.

Key Words. Poly(aryl ether ether ketone) (PEEK) for high temperature gas and vapor membrane applications; Effects of rolltrusion processing on transport and separation in PEEK

* To whom correspondence should be addressed.

INTRODUCTION

Operating costs in both pervaporation and vapor permeation separations depend significantly upon the permeate condenser temperature. Since most of these applications require condenser temperatures below ambient and hence, expensive refrigeration and vapor compression technology, operating costs can be substantial. By raising the condenser temperature 30 to 50°C above ambient, low cost air-cooled condensers may be substituted, so that considerable capital and operating cost savings can be realized. However, raising the condenser temperature implies a concommitant increase in the feed side temperature. For example, in the pervaporation or vapor permeation of azeotropic water/ethanol mixtures, feed side temperatures in excess of 150°C would be necessary to deliver >99.5% ethanol with a permeate condenser operating at >50°C. The problem is that the nonporous polymeric membranes available today lack the degradative stability and/or mechanical integrity necessary for use at temperatures in excess of ~130 to 150°C and/or in harsh chemical environments (1). Although a number of engineering plastics can be utilized at temperatures in excess of 150°C in demanding chemical environments, they are unavailable as membrane materials because they are not amenable to solution-based membrane-forming technologies (2).

The semicrystallizable aromatic engineering polymer, poly(aryl ether ether ketone) or PEEK, has been found to possess superior thermal/mechanical stability as well as resistance to hydrolytic and chemical attack at temperatures in excess of 200°C. However, PEEK and other high performance polymers are usually intractable or require solvents that are generally characterized as noxious and/or flammable, and temperatures of 250 to 350°C are needed to achieve appreciable dissolution (3–5). Hence, fabrication of ultrathin films is difficult. Interestingly, the need for ultrathin films less than 1 to 5 μm in thickness, for instance, is alleviated to some extent not only by (i) the high permeabilities and selectivities encountered in high temperature vapor and liquid membrane separations but also by (ii) the reduced capital and operating costs associated with the permeate condensers. For these membrane applications, novel rolltrusion solid-state processing technology (6, 7) can now be used effectively to generate rugged permselective membranes from solvent-resistant, commercially available, engineering polymers.

In several recent papers (8–11) the influence of the rolltrusion processing temperature and draw ratio on the transport and selectivity of gases in isotactic polypropylene (iPP) has been detailed. It has been demonstrated that rolltrusion processing generally improves membrane selectivity (11) based upon penetrant size, but in some instances reduces the

permeability (8–10). However, because of the unique process-induced morphological features, the maximum ca. 7-fold drop in gas permeability observed in rolltruded iPP is much smaller than the ca. 10 to 1000-fold decline reported in uniaxially drawn films of similar polymers formed at comparable draw ratios (12–15). In addition, macrovoid formation created via crazing (stress whitening) or induced through rolltrusion processing has been demonstrated, for instance, to improve gas permeability in iPP without sacrificing membrane selectivity (10, 11).

In the current study the effects of rolltrusion processing on the transport and selectivity of several gases (H_2, CO_2, N_2, and CH_4) and vapors (H_2O and ethanol) in PEEK over temperatures ranging from 40 to 200°C have been determined. Although solvent uptake and swelling of PEEK at temperatures to ca. 100°C have been investigated in recent years (16–22), these studies have been focused primarily upon the effects of penetrant sorption on the physical properties of this polymer. Consequently, little consideration has been given to its possible use as a membrane material until now. Applications of PEEK membranes have been limited to room temperature micro- and ultrafiltration separations (3, 4). In this paper we demonstrate that films of rolltruded PEEK can be used successfully for the separation of gases and more especially vapors at temperatures well in excess of 100°C.

THEORY

The flux of gases, vapors, and liquids through nonporous polymers can be described by the three-step solution-diffusion model. One-dimensional component fluxes can be determined using (23)

$$J_i = -D_i s_i \frac{\partial f_i}{\partial z} \tag{1}$$

where D_i is the diffusion coefficient, f_i is the fugacity, and s_i is the solubility of penetrant i in the membrane. The overall transport of material across a membrane is termed the permeability which is defined as

$$P_i = \frac{J_i h}{(p_{i,f} - p_{i,p})A} \tag{2}$$

where p_i is the partial pressure of component i, A is the membrane area, h is the membrane thickness, and the subscripts "f" and "p" indicate the feed and permeate side of the membrane, respectively.

For an ideal system in which the polymer does not interact with the penetrant, $f_i = p_i$, and D_i and s_i are independent of penetrant concentration. Under these conditions Eqs. (1) and (2) can be combined so that P_i

is the product of D_i and s_i. Ideal behavior is typical of permanent gases in polymers at temperatures above T_g, and estimates of P_i, D_i, and s_i can be made using the time lag method already described elsewhere (24).

Nonideal systems are characterized by concentration and/or time-dependent transport coefficients which are typical of vapor and liquid transport through polymers. Estimating any of the transport coefficients using the time lag method (24) is difficult and can be accomplished only when (i) a model equation for the D_i and s_i is assumed and (ii) the transport coefficients are independent of time. Details specific to each vapor considered in this study (H_2O and EtOH) are given later.

Penetrant transport generally occurs through the amorphous phase of the polymer. In semicrystalline polymers the diffusivity and solubility are often normalized by the amorphous volume fraction, α_a, so that

$$s = \alpha_a s_a \tag{3}$$

and

$$D = \alpha_a D_a \tag{4}$$

where s_a and D_a are the solubility and diffusivity in the amorphous material (component subscripts have been dropped for brevity). Since all of the PEEK films considered in this study are semicrystalline, we report only amorphous transport coefficients.

Significant variations in the polymeric morphology arise through rolltrusion processing. The amorphous chain immobilization (or chain stiffness) constant, β, and the diffusive pathway tortuosity, τ, are two empirical factors that are employed to relate changes in the transport behavior and properties to variations in the polymer morphology.

Based upon the molecular theory of diffusion of Pace and Datyner (25, 26), it is reasonable to assume a correspondence between the activation energies and β. Therefore, as in previous papers (9–11), changes in the activation energies of each penetrant in rolltruded PEEK are used to assess the effect of processing on β.

The tortuosity represents the added diffusive path length of a penetrant resulting from circumvention of impermeable regions in the polymer, such as crystallites. As a result of solid-state processing, the crystallinity as well as the crystallite size, distribution, and orientation can be significantly altered, thereby influencing τ. Relatively impermeable amorphous regions that are also created via solid-state processing have been invoked to explain changes in the transport coefficients of rolltruded (9–11) and other solid-state processed films (12–15) that exceed those changes predicted by variations in the activation energies and the crystallinities encountered in this research. To account for the added diffusive pathlength, Eq. (4)

becomes

$$D = \frac{\alpha_a D_a}{\tau} \tag{5}$$

It is known that the ability of a membrane to separate components from a mixture is given by the actual separation factor

$$\alpha_{i,j}^{\text{actual}} = \frac{x_i/x_j}{y_i/y_j} \tag{6}$$

where x_i and y_i are the feed and permeate concentrations of component i, respectively. In the ideal system this reduces to a ratio of the permeabilities of the fast to slow gas, or

$$\alpha_{i,j}^{\text{ideal}} = \frac{P_i}{P_j} \tag{7}$$

Differences between the actual and ideal separation factors are not uncommon and can be traced to nonideal penetrant/penetrant or polymer/penetrant interactions. The extent of these interactions can be assessed by examining deviations of the mixture permeability (P_i^{mix}) from the pure component permeability (P_i) of component i. The P_i^{mix} can be determined using

$$P_i^{\text{mix}} = \frac{y_i}{x_i} P_{\text{tot}}^{\text{mix}} \tag{8}$$

where $P_{\text{tot}}^{\text{mix}}$ is the total mixture permeability.

EXPERIMENTAL

Film Preparation

Samples of amorphous PEEK were obtained in sheet form from ICI, Wilton, UK. The sheets were annealed under tension at 210°C for 2 hours to induce crystallization and to remove internal stresses. Two annealed films were rolltruded at processing temperatures of 230 and 285°C to a draw ratio* (DR) of approximately 4 using the rolltrusion apparatus described elsewhere (6, 7). The properties of the rolltruded and an unprocessed (annealed) film are given in Table 1. Experimental density determinations were made using a density gradient column of EtOH and chloroform at 25°C. Measurements of the sample mass before and after the density determinations revealed undetectable uptake of either EtOH

* The draw ratio is calculated as the ratio of the initial cross-sectional area of the film to the final cross-sectional area after rolltrusion.

TABLE 1
Pertinent Characteristics of the PEEK Films Used in This Study

T_p (°C)	DR (—)	ρ (g/cm³)	α_a (—)	%TM[b]
NA[a]	1.0	1.2915	0.87	0
230	3.7	1.3039	0.65	350
285	4.0	1.3070	0.68	320

[a] Unprocessed annealed film.
[b] Percent improvement in the tensile modulus compared with the unprocessed film. Measurement temperature is 80°C.

or chloroform. From the density, amorphous volume fractions were estimated using the equation

$$\alpha_a = 12.8205/\rho - 9.154 \quad (9)$$

due to Blundell and Osborn (27).

Permeation/Separation Factor Measurements

The PEEK films were installed in the permeation cell as described elsewhere (8). The amorphous transport coefficients, P_a, D_a, and s_a, for several pure gases (H_2, CO_2, N_2, and CH_4 [>99.9%]) and vapors (deionized H_2O and anhydrous ethanol [EtOH]) and mixtures of CO_2/N_2 (26.4 vol% CO_2) and H_2O/EtOH (39.1, 11.6, and 7.6 wt% H_2O in the vapor phase) were determined at temperatures in the range of 40 to ca. 180°C. We have previously conducted studies to 225°C with H_2, N_2, and CO_2 in rolltruded PEEK (8).

Gas permeation experiments were conducted at 75 psia, since little penetrant pressure dependence of the transport coefficients was noted in the range of 20 to 200 psia above and below the glass transition of the polymer. Pure component and mixed vapor permeation experiments were performed under saturated and superheated conditions. Since the permeate pressure was kept below 10 torr for all of the experimental runs, $p_{i,p}$ was assumed to be low enough to be neglected in the determination of the permeability using Eq. (2). A Hewlett-Packard 5880A series gas chromatograph was utilized to determine the feed and permeate compositions, so that actual separation factors could be obtained.

The permeation apparatus and its operation are discussed elsewhere (8). An external thermostatted feed tank (T_{max} = 170°C, control: ±0.3°C) and a liquid N_2 trap for permeate collection have been added to permit saturated and superheated vapor experiments to be conducted.

RESULTS

Permeation

The permeation temperature dependence of the amorphous permeabilities and, if obtainable,* the diffusivities and solubilities of the pure gases in the annealed and rolltruded PEEK films are shown in Figs. 1, 2, and

* Diffusivities and solubilities were not obtained in some instances because the time lags were too short.

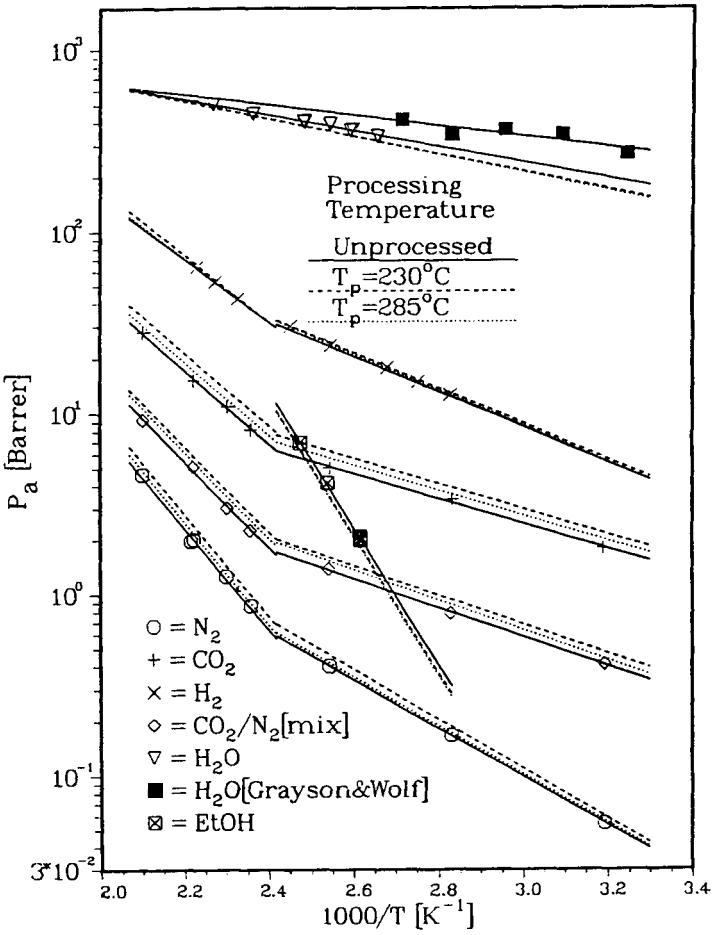

FIG. 1 Amorphous permeabilities plotted as a function of inverse temperature in unprocessed and rolltruded PEEK.

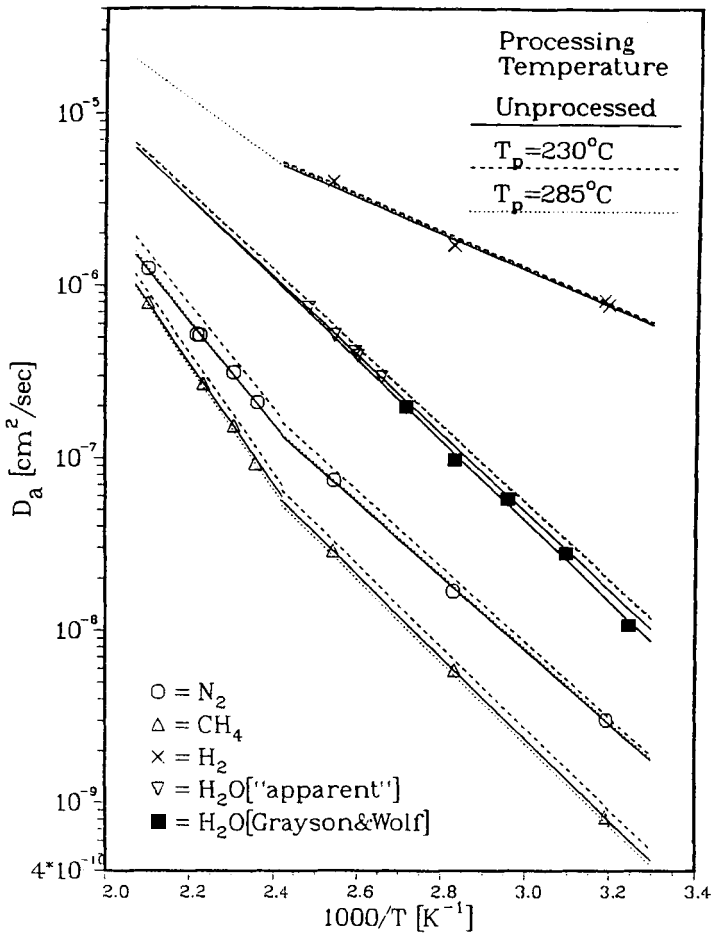

FIG. 2 Amorphous diffusivities plotted as a function of inverse temperature in unprocessed and rolltruded PEEK.

3, respectively. To reduce the clutter in these figures, the actual data points are shown only for the unprocessed film for each penetrant. The remaining data points for the films processed at 230 and 285°C are illustrated by best line fits only. Figure 1 also displays the amorphous permeabilities of saturated water and ethanol vapor in the various PEEK films.

The effect of feed vapor activity on the transport of water in PEEK was also examined. Figure 4 shows the permeability and the normalized

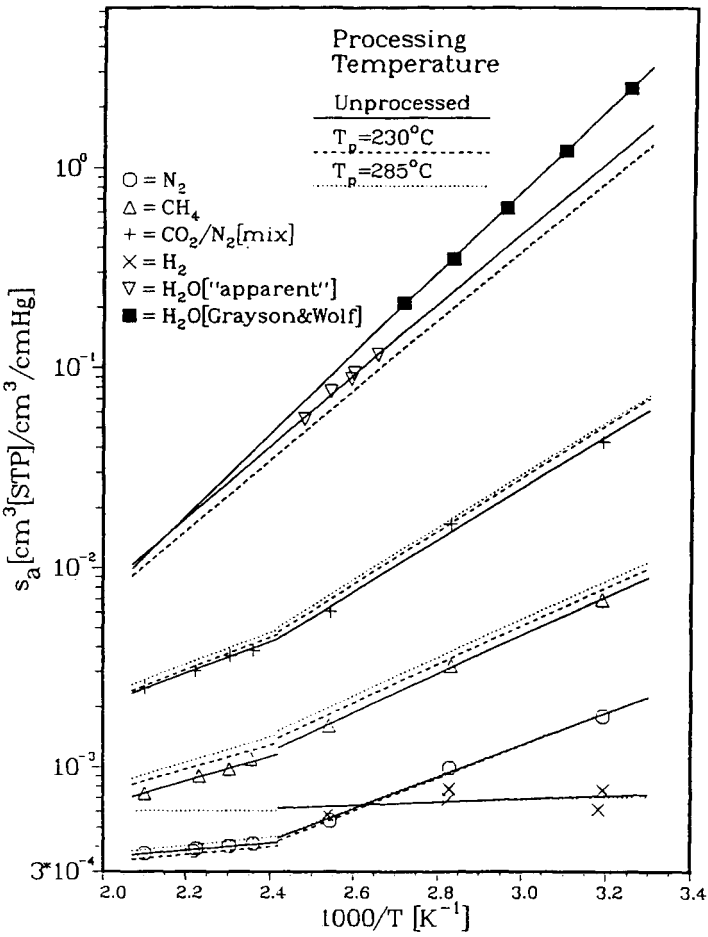

FIG. 3 Amorphous solubilities plotted as a function of inverse temperature for unprocessed and rolltruded PEEK.

reciprocal time lags ($h^2/6L_t$) of H_2O plotted as a function of feed vapor activity (p/p_{sat}) for unprocessed (U) and rolltrusion processed (P) PEEK at permeation temperatures of 130 and 160°C. The concentration dependence of the time lags hinders the determination of the actual diffusivities (and solubilities) of water in PEEK. However, throughout this paper, the D_a and s_a for H_2O vapor are approximated from these time lags and are reported as "apparent" values. Apparent diffusivities and solubilities of

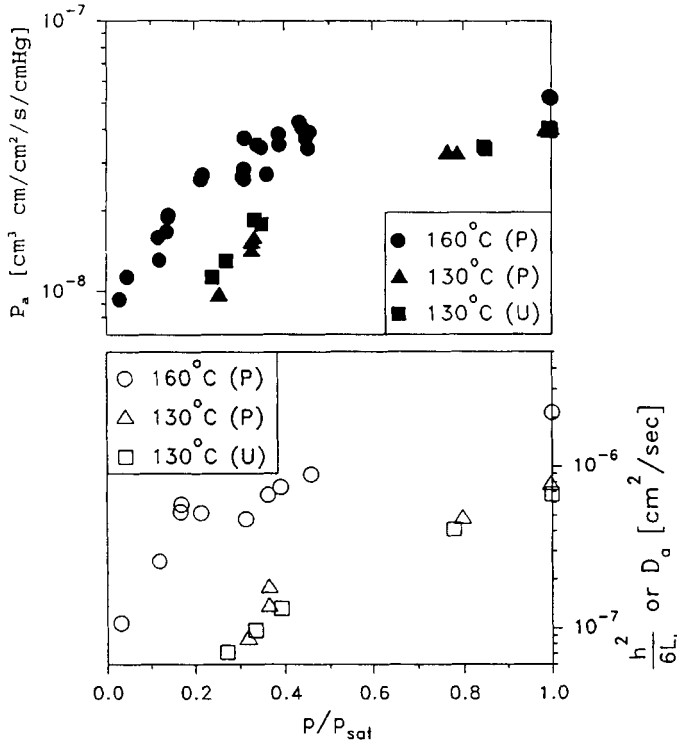

FIG. 4 Permeabilities and normalized time lags (L_t) or apparent diffusivities of water vapor plotted as a function of feed activity (p/p_{sat}) for rolltruded and unprocessed PEEK.

saturated water vapor are plotted in Figs. 2 and 3 for comparison with the gases. Grayson and Wolf (16) have also studied the transport of H_2O in PEEK via liquid immersion studies, and their data are also plotted in Figs. 1 to 3.

Compared with gas and water vapor, the permeation of EtOH vapor is considerably more complicated. Figure 5 shows typical time lag plots for EtOH at various temperatures in PEEK rolltruded at 285°C. Note that the abscissa is a reduced time scale expressed as the ratio of the actual over the total experimental run time. Total experimental run times for each permeation temperature are given in Fig. 5. For all permeation temperatures, the permeability (proportional to the slope) is initially low and remains relatively constant up to some induction time, t_i. At this stage a

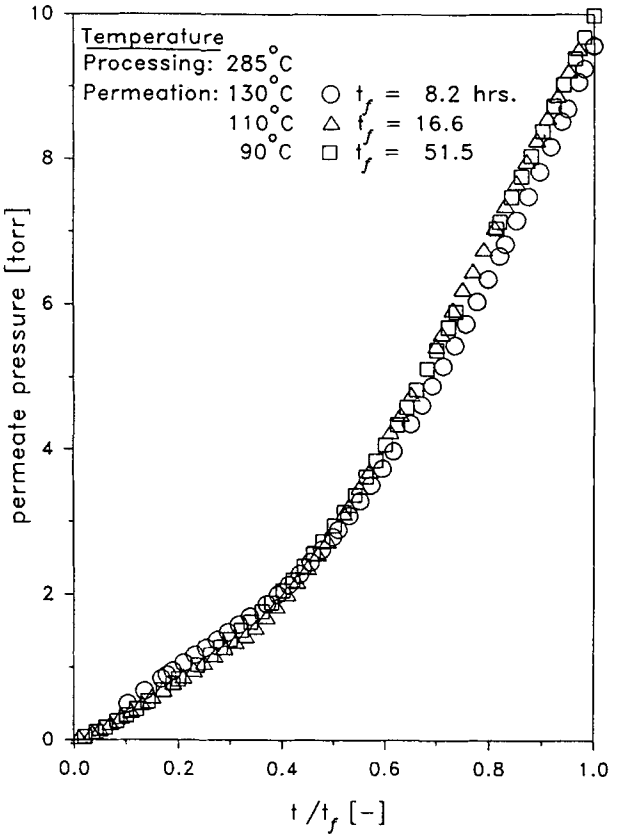

FIG. 5 Normalized time lag plots for ethanol in PEEK rolltruded at 285°C. The kink in each plot corresponds to the induction time, t_i.

step increase in the permeability is observed. The permeabilities of EtOH reported in Fig. 1 were determined from the slope of the data at times greater than t_i in Fig. 5. However, since time lags cannot be obtained from Fig. 5, "apparent" diffusivities and solubilities for EtOH in PEEK are not reported.

From the slopes of the data in Figs. 1 to 3, permeation and diffusive activation energies (E_p and E_d) and heats of solution (ΔH_s) were evaluated and are given in Table 2 for each film at permeation temperatures above and below T_g. This temperature agrees well with the glass transition tem-

TABLE 2
Values of E_d and ΔH_s in Unprocessed and Rolltruded PEEK. E_p's for EtOH Are Also Listed for the Other Penetrants, E_p Can Be Determined from $E_p = E_d + \Delta H_s$

E_d (kJ/mol)	$<T_g$, T_p = NA[a]	T_p = 230	T_p = 285	$>T_g$, T_p = NA[a]	T_p = 230	T_p = 285
N_2	41.3	41.9	41.3	57.4	57.9	58.6
CO_2	38.2	38.9	38.6	55.8	55.9	56.1
CH_4	45.5	45.4	45.5	67.5	67.1	68.8
H_2	20.1	20.0	20.5	—[b]	—	33.7
H_2O	43.3	42.9	42.9	43.3	42.9	42.9

ΔH_s (kJ/mol)	$<T_g$, T_p = NA[a]	T_p = 230	T_p = 285	$>T_g$, T_p = NA[a]	T_p = 230	T_p = 285
N_2	−15.3	−15.6	−15.1	−3.5	−3.8	−4.0
CO_2	−24.9	−25.4	−25.2	−15.0	−15.6	−15.2
CH_4	−18.6	−18.6	−18.4	−11.8	−11.6	−12.0
H_2	−1.5	−0.3	−1.6	—	—	−0.1
H_2O	−34.3	−33.7	−33.6	−34.3	−33.7	−33.6

E_d (kJ/mol)	$<T_g$, T_p = NA[a]	T_p = 230	T_p = 285	$>T_g$, T_p = NA[a]	T_p = 230	T_p = 285
EtOH	72.7	72.9	73.3	—	—	—

[a] Unprocessed PEEK film.
[b] Data unavailable.

perature of 148°C for PEEK as measured by DSC in our labs. No such "break" in the transport coefficients is observed for H_2O, and pure component data are not available for EtOH permeation above the T_g of PEEK.

To characterize better the influence of rolltrusion processing on the gas and vapor transport coefficients, the "X-fold" changes in the P_a, D_a, and s_a of rolltruded compared to unprocessed PEEK are plotted as a function of permeation temperature in Figs. 6, 7, and 8, respectively. This convention has been adopted in previous papers (10, 11) so that increases or decreases in the transport coefficients of equal magnitude appear as equivalent deflections (though opposite in direction) from the baseline value of 1.0, which represents the unprocessed film. The small step in several of the curves between 140 and 150°C corresponds to the glass transition temperature. Additionally, the symbols in Figs. 6 to 9 do not represent individual data points, but instead are used as simple visual aids or markers for each penetrant.

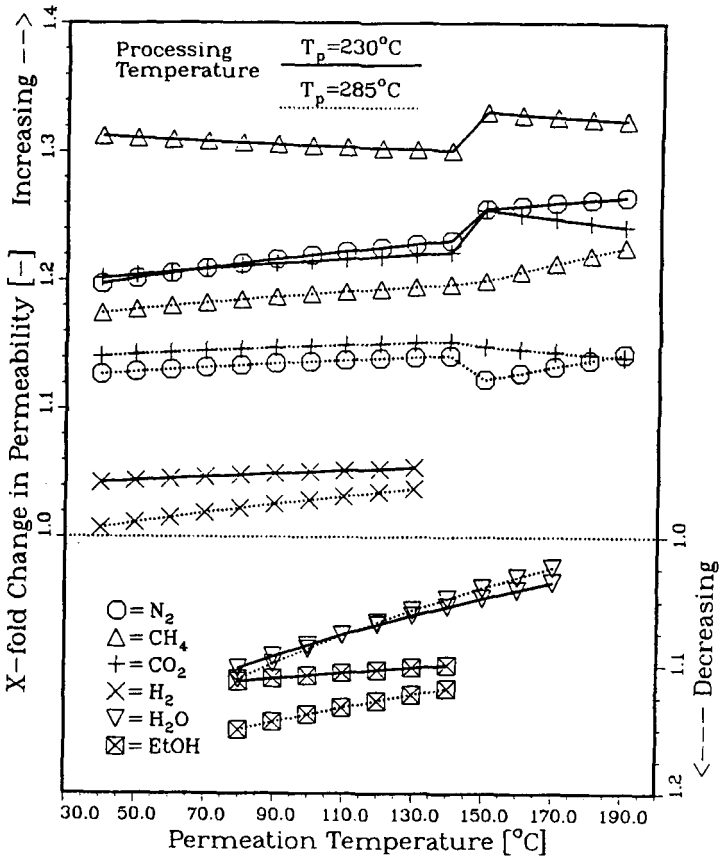

FIG. 6 X-fold change in the gas and vapor permeability of the rolltruded films compared to the unprocessed film plotted as a function of permeation temperature.

Separation Factors

Ideal and actual separation factors for the CO_2/N_2 system are shown in Fig. 9. The ideal values have been determined from the pure component permeabilities of Fig. 1. Differences between the $\alpha_{i,j}^{ideal}$ and $\alpha_{i,j}^{actual}$ can be attributed to deviations of the mixture permeability of component i, P_i^{mix}, from its pure component value, P_i. Figure 10 shows these deviations plotted as the "X-fold" changes (denoted ΔP_i) of $P_{N_2}^{mix}$ and $P_{CO_2}^{mix}$ from the pure component values for the unprocessed and rolltruded PEEK films.

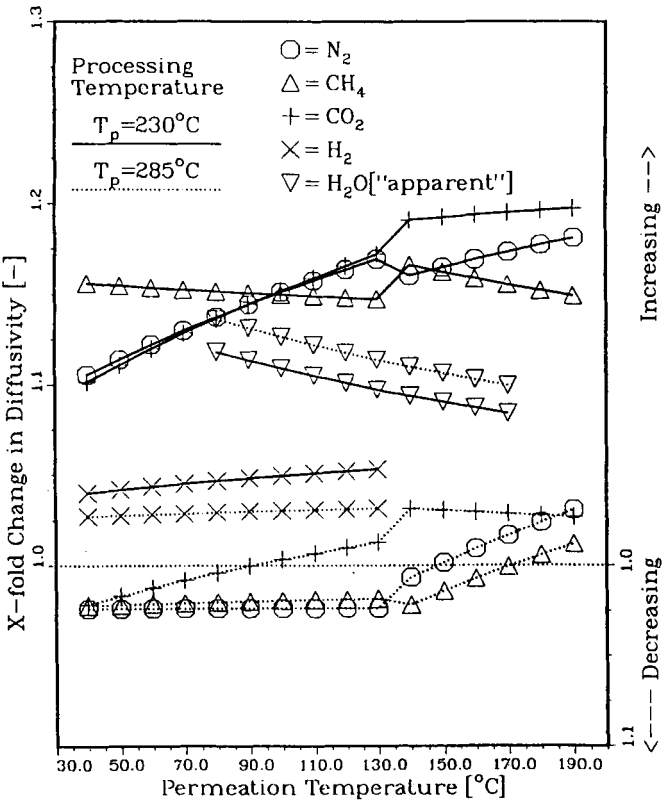

FIG. 7 X-fold change in the gas and vapor diffusivity of the rolltruded films compared to the unprocessed film plotted as a function of permeation temperature.

Note that the mixture permeability of CO_2 declines by ca. 1.3-fold in comparison with its pure component value; no change is observed for N_2.

The ideal H_2O/EtOH separation factors, $\alpha^{ideal}_{H_2O,EtOH}$, are also given in Fig. 9. These have been calculated from the saturated vapor permeabilities given in Fig. 1. Values for $\alpha^{ideal}_{H_2O,EtOH}$ above the T_g of PEEK have been estimated assuming that the permeation activation energy, E_p, of EtOH is invariant above and below T_g. Although this is unlikely, such an approximation gives the maximum expected value of $\alpha^{ideal}_{H_2O,EtOH}$ at temperatures

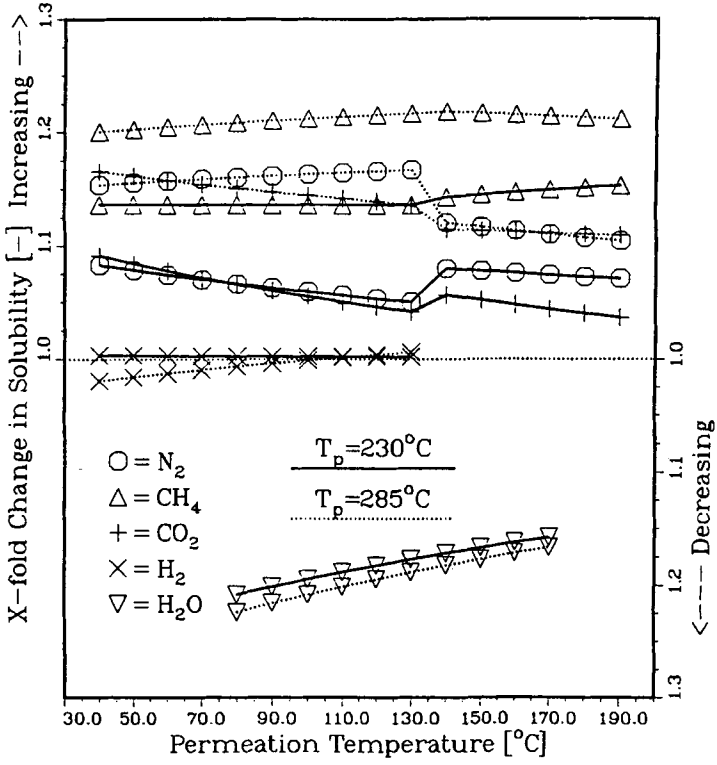

FIG. 8 X-fold change in the gas and vapor solubility of the rolltruded films compared to the unprocessed film plotted as a function of permeation temperature.

greater than the T_g of PEEK and is useful for comparing ideal and actual separation factors. The actual separation factors, $\alpha^{actual}_{H_2O,EtOH}$, are given in Fig. 9 and Table 3, and have been determined for permeation temperatures of 130 and 160°C in the unprocessed film and the film rolltruded at T_p = 285°C. All vapor mixture separation runs made at 130°C were performed at the saturation pressure of the mixture, whereas the run at 160°C was conducted at $p/p_{sat} \approx 0.67$. Table 3 also contains the actual permeabilities of each component in the mixture (P_i^{mix}) calculated from Eq. (8) and the

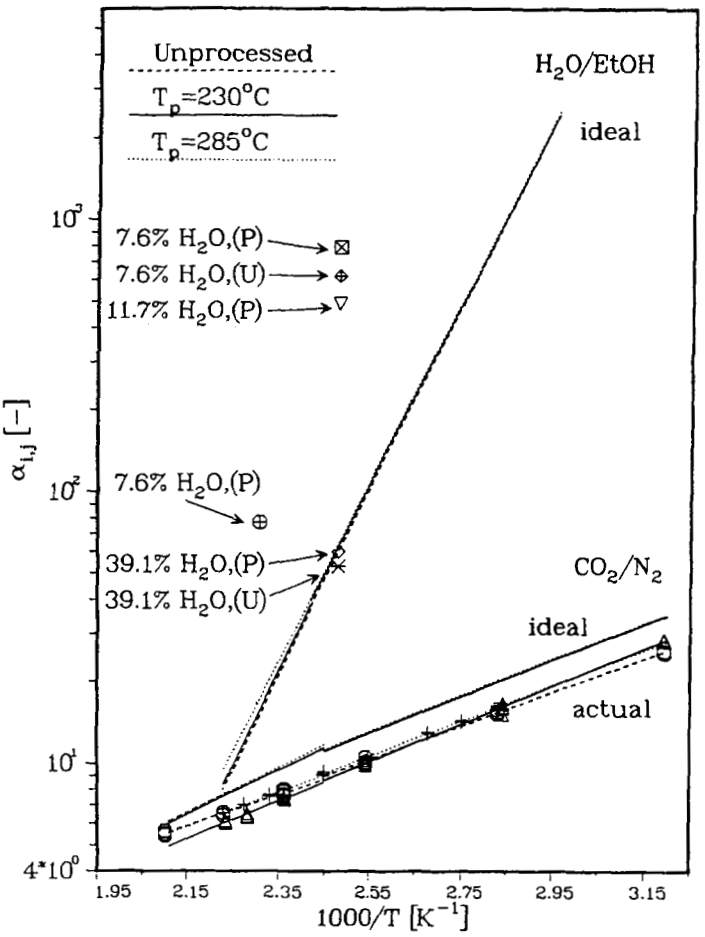

FIG. 9 Ideal and actual separation factors plotted as a function of inverse temperature for CO_2/N_2 and H_2O/EtOH systems in unprocessed and rolltruded PEEK.

permeabilities of saturated H_2O and EtOH vapor P_i^{sat} from Fig. 1. Table 3 also contains the permeability of H_2O at a vapor pressure which corresponds to the partial pressure of H_2O in the mixture, $P_{H_2O}^{vp}$ (as opposed to the saturated vapor permeabilities, see Fig. 4).

TABLE 3
Actual Separation Factors for Several Feed Concentrations of H_2O in EtOH for Rolltruded and Unprocessed PEEK. Also Given Are the Mixture Permeabilities (P^{mix}) and Saturated Vapor Permeabilities (P^{sat}) for Both Penetrants. The Permeability of H_2O in PEEK at a Vapor Pressure Comparable to That of the Mixture Is Given by $P^{vp}_{H_2O}$

T_p (°C)	T_d (°C)	$X^{feed}_{H_2O}$ (wt%)	$\alpha^{actual}_{H_2O,EtOH}$ (—)	$P^{mix}_{H_2O}/P^{mix}_{EtOH}$ (barrer)	$P^{sat}_{H_2O}/P^{sat}_{EtOH}$ (barrer)	$P^{vp}_{H_2O}$ (barrer)
285	130[a]	39.1	60	204/3.38	385/6.02	~230
285	130	11.6	490	232/0.47	385/6.02	~100
285	130	7.6	790	331/0.42	385/6.02	~80
285	160	7.6	89	374/4.23	520/NA[b]	~120
U[c]	130	39.1	53	223/4.42	407/6.8	~230
U	130	7.6	590	394/0.67	407/6.8	~80

[a] Permeation temperature.
[b] Data not available.
[c] Unprocessed PEEK film.

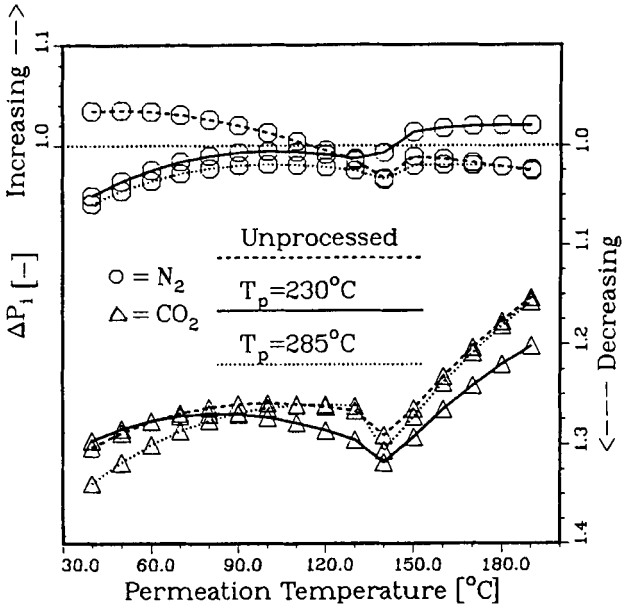

FIG. 10 Differences between the mixture and pure component permeabilities of the CO_2/N_2 mixture in unprocessed and rolltruded PEEK.

DISCUSSION

Unlike isotactic poly(propylene) (9–11), Figs. 1 to 9 show that the gas and vapor transport properties and the selectivity of PEEK are only slightly altered under the rolltrusion conditions employed here. In Table 4 changes in the transport properties of N_2 in rolltruded PEEK are compared to rolltruded iPP for a similar processing temperature range and draw ratio. Variations in the transport properties of iPP resulted from changes in the polymer morphology due to rolltrusion (9, 10). These included changes in the microvoid content, diffusive pathway tortuosity (associated with crystallinity changes, crystallite orientation, and the formation of impermeable amorphous regions), and amorphous chain stiffness. Although more subtle, these morphological changes are consistent with the observed variations in the transport properties of PEEK.

Gases

Figure 8 shows that rolltrusion can improve gas solubility by as much as 30% in PEEK, which is comparable with the increases observed in rolltruded iPP (9, 10). A large uniform increase in the average amorphous chain separation is unlikely to account for this change, since it would result in significant reductions in the activation energies, E_d and ΔH_s. Instead, microvoids may be induced in the rolltruded PEEK sample as adduced and confirmed already for iPP (9, 10). However, it is unlikely that the general improvement in the s_a as the "processing temperature"

TABLE 4
Comparison of the Changes in Selected Transport Properties of Rolltruded PEEK and iPP (10) for Permeation Temperatures above the T_g. Draw Ratio Is ca. 4 in All Films

	PEEK		iPP	
	T_p = 285°C	T_p = 230°C	T_p = 125°C	T_p = 50°C
E_d (kJ/mol)[a]	−0.4	+0.7	+5.0	+4.7
ΔH_s (kJ/mol)[a]	−0.2	+0.2	−3.1	+0.2
D_a (cm²/s)[b]	NC[c]	1.20 ↑	1.6 ↓	6.7 ↓
S_a (cm³{stp}/cm³/s)[b]	1.21 ↑	1.15 ↑	1.7 ↑	1.2 ↑

[a] Activation energies are given as the difference between the rolltruded and original film (i.e., rolltruded − original).

[b] D_a and s_a given as X-fold change. Arrow indicates increase or decrease.

[c] No change.

is raised (see Fig. 8) is due to a simultaneous increase in microvoid content. On the contrary, previous results with rolltruded iPP (9, 10) [as well as the general temperature dependence of macrovoid formation via crazing in iPP, PEEK, and other polymers (28)] indicate that the formation of voidlike defects is actually reduced as the processing temperature is raised. Therefore, variations in the amorphous chain stiffness and/or the fraction of impermeable amorphous material, not microvoid formation, probably accounts for the processing temperature dependence of the s_a as discussed below.

The negligible size dependence of the improvement in the D_a of N_2, CO_2, and CH_4 following rolltrusion at processing temperatures of 230 and 285°C (see Fig. 7) and the small variations in the activation energies (see Table 2) indicate that the amorphous chain stiffness associated with diffusive transport increases only marginally at the two processing temperatures considered to date, hence this result suggests that the formation of impermeable amorphous regions accounts for the processing temperature dependence of s_a. We have shown already (9, 10) that the fraction of impermeable amorphous material increases as the processing temperature is lowered in rolltruded iPP (9, 10). A similar temperature dependence is expected in PEEK,* and this would be expected to yield a reduction in the s_a as the processing temperature is lowered. This is consistent with the observed trend in Fig. 8.

An increase in the fraction of relatively impermeable amorphous material with decreasing processing temperature, however, is expected to produce a concomitant rise in the tortuosity, τ, and drop in the D_a. This result contrasts with the improvement in the D_a as the processing temperature is increased as illustrated in Fig. 7. There are two likely sources for this trend, namely, (i) microvoid formation and/or (ii) increased crystallite orientation [which reduces the τ (10)]. Both factors would be expected to improve the D_a. Additionally, the predicted temperature dependence of each factor (9, 10) is consistent with the trend in the D_a displayed in Fig. 7.

Vapors

The P_a of H_2O vapor in PEEK declines following rolltrusion over the entire range of vapor pressures considered as shown in Figs. 4 and 6. The P_a of saturated EtOH vapor is similarly depressed (Fig. 6). The data in Figs. 7 and 8, respectively, suggest that the reduction in the P_a of water

* More extensive measurements will be made over a wider span of processing conditions to resolve this trend.

vapor results from a drop in the apparent s_a, which is correspondingly larger than the observed increase in the apparent D_a.

Since the s_a of the gases increased following rolltrusion, this drop in water vapor solubility is unexpected. However, water is expected to be a more efficient plasticizer of PEEK than the gases studied in this work. It seems that rolltrusion enhances polymer stability and at the same time hinders the ability of H_2O to plasticize PEEK, and hence this is responsible for the reduced s_a values.

The apparent D_a of H_2O, shown in Fig. 7, increases as a consequence of rolltrusion processing. An increase in the microvoid content and a decrease in the tortuosity (due to crystallite orientation) most likely contribute to this improvement in D_a, as observed for the gases.

Grayson and Wolf (16) studied the sorption of liquid water in semicrystalline, unoriented PEEK for permeation temperatures ranging from 35 to 95°C. Considering that the driving forces for saturated water vapor and liquid water permeation are equivalent at constant temperature (equivalent activity), the 15 to 20% discrepancy shown in Fig. 1 between their data and ours is somewhat unexpected. However, large differences between vapor and liquid permeabilities have been reported in other polymer/penetrant systems (29) due to differences in the plasticizing capabilities of solvent vapors and liquids.

Anomalous Permeation of EtOH

Determination of the apparent diffusivities and solubilities of ethanol in PEEK was impossible using the time lag method because of the time-dependent nature of the permeation. The sharp increase in EtOH flux shown in Fig. 5 is indicative of Fickian Case II sorption kinetics (30). Case II kinetics are identified by a step change in the concentration profile (termed the "front") of the penetrant in the polymer. Ahead of the front, penetrant transport is controlled by normal Fickian diffusion into the unswollen polymer. However, behind the diffusion front, the polymer is swollen, producing a significant enhancement in the permeability of the penetrant. Since the front advances with time through the polymer, the permeability exhibits a step change at some induction time, t_i, as observed for EtOH in Fig. 5. Similar kinetics have been observed with other organic liquids (CH_2Cl_2, $CHCl_3$, toluene, benzene) during sorption experiments in PEEK (17, 18).

Case II kinetics have been associated with depression of the glass transition temperature, T_g, of the polymer below the experimental permeation temperature by the penetrant (16, 30). A rough estimate of the dependence of the glass transition temperature of a polymer on penetrant concentra-

tion can be made using the Fox (31) equation given by

$$\frac{1}{T_{g,r}} = \frac{w_p}{T_{g,p}} + \frac{w_s}{T_{g,s}} \tag{10}$$

where $T_{g,r}$, $T_{g,p}$, and $T_{g,s}$ are the glass transition temperatures of the swollen polymer, the pure polymer, and the penetrant, respectively, and w_p and w_s are the weight fractions. Values for $T_{g,s}$ of small molecules can be obtained from Fedors (32), and the T_g of PEEK is ca. 148°C. Grayson and Wolf (16) used this equation to estimate the weight fraction of benzene and toluene necessary to depress the glass transition temperature of amorphous PEEK below the experimental sorption temperature of 95°C. The calculated weight fractions correlated well with the observation of a transition from Case II to Case I kinetics during desorption of these organic liquids from PEEK (16).

This equation may be used to account for the differences in permeation kinetics of EtOH and H_2O. Unfortunately, we cannot obtain the solubility of EtOH in PEEK from the time lag plots. Nevertheless, Fig. 11 shows that a linear relationship exists between the s_a and the Lennard–Jones potential, ϵ/k, of several penetrants in unprocessed PEEK for a permeation temperature of ca. 100°C. From this figure the solubility of EtOH in PEEK is estimated as 0.45 $cm^3[STP]/cm^3/cmHg$ given that the (ϵ/k) of

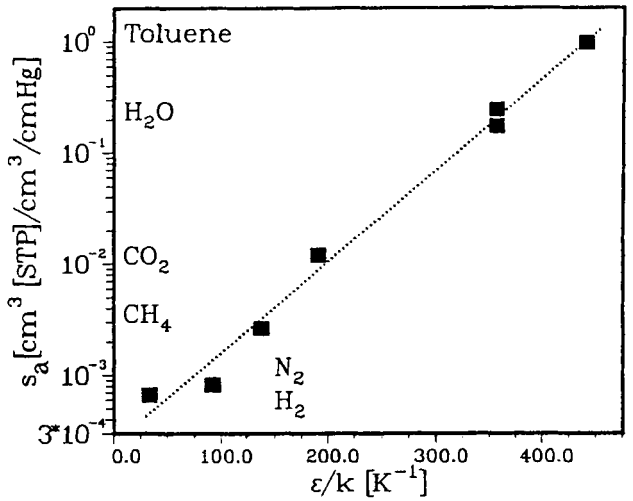

FIG. 11 Dependence of the gas and vapor solubility on penetrant Lennard–Jones parameter in unprocessed and rolltruded PEEK at ca. 100°C.

EtOH is ca. 391 K (33). According to Eq. (10), a solubility of only 0.15 $cm^3[STP]/cm^3/cmHg$ (3.6 wt%) is necessary to depress the glass transition temperature of PEEK below 100°C, in accordance with the observation of Case II kinetics. In contrast, water solubility of ca. 1.2 $cm^3[STP]/cm^3/cmHg$ (5.8 wt%) is needed to depress the T_g of PEEK below 100°C. From Fig. 3 the apparent solubility of H_2O in PEEK at this temperature is significantly lower based upon our data and that of Grayson and Wolf, so that Case II kinetics are neither predicted nor observed for this penetrant.

Separation Factors

Figure 9 shows that the actual separation factors for the CO_2/N_2 mixture are depressed relative to their ideal values. This is attributed to a decrease in the mixture permeability of CO_2 ($P^{mix}_{CO_2}$) compared with its pure component value as displayed in Fig. 10. As established in iPP (11), a reduction in the $P^{mix}_{CO_2}$ in PEEK may be influenced by the presence of N_2 which suppresses (or "screens") CO_2 plasticization of PEEK. Variations in the processing conditions in this investigation do not appear to influence significantly the separation factors, which is not unexpected considering the marginal influence of the effect of processing conditions on the gas transport coefficients.

In comparison, the $\alpha^{actual}_{H_2O,EtOH}$'s are enhanced substantially at water vapor concentrations of 7.6 and 11.7 wt% as shown in Fig. 9 for the unprocessed and rolltruded films. The data in Table 3 indicate that these improvements result from large decreases in the P^{mix}_{EtOH} compared with the P^{sat}_{EtOH}. The sharp drop in the P^{mix}_{EtOH} at 130°C may result from a reduction in the solubility of EtOH in PEEK below the threshold value needed to depress the T_g below the permeation temperature. Hence, the two-stage permeation associated with Case II diffusion is no longer realized, so that the permeability of EtOH never increases above its value before the induction time shown in Fig. 5.

In contrast with the P^{mix}_{EtOH}, the $P^{mix}_{H_2O}$ decreases only slightly compared with the $P^{sat}_{H_2O}$ and increases dramatically with respect to the permeability of pure H_2O at the same vapor pressure, $P^{vp}_{H_2O}$, as shown in Table 3 for the unprocessed and rolltruded films. Interestingly, the $\alpha^{actual}_{H_2O,EtOH}$ also increases as the concentration of H_2O in the mixture decreases, which is due exclusively to the improvement in the $P^{mix}_{H_2O}$ (see Table 3). The improvement in the $P^{mix}_{H_2O}$ versus its pure component permeability at a comparable vapor pressure, $P^{vp}_{H_2O}$, and its concentration dependence may result from two likely sources, namely,

1. An increase in the diffusivity of H_2O due to plasticization of the PEEK by EtOH and/or

2. A disruption in the "clustering" of H_2O due to a combination of lower vapor activity and the presence of EtOH

Comparison of PEEK to Other Polymers for Vapor Separation

The removal of small amounts of H_2O (<10 wt%) from EtOH and other organic compounds via vapor permeation has been investigated by several authors (34–39). Vapor permeation offers several advantages over the more common pervaporation technique (38, 39). Several of these are

1. No concentration polarization and a more favorable flow distribution
2. Simpler module design since the heat of evaporation need not be supplied
3. Isothermal operation

Furthermore, process streams contaminated with water are in many cases high temperature (>80°C) vapor streams from distillation columns and reactors, so that vapor permeation would be more advantageous in terms of thermal efficiency and hence process economics.

Table 5 shows typical values of the vapor permeability of H_2O and $\alpha^{actual}_{H_2O,EtOH}$ for several polymers (34–37) at various feed temperatures and concentrations. In general, results for PEEK membranes compare favorably with other membranes from a permeability and selectivity standpoint

TABLE 5
Vapor Permeabilities of H_2O and Actual Separation Factors for H_2O/EtOH Mixtures for Various Polymers Compared with PEEK Considered in This Study

Polymer	T (°C)	Composition	P_{water} (barrer)	$\alpha_{H_2O,EtOH}$
PVA/PAN Composite (35, 36)	85	10 wt% H_2O in EtOH	~2260[a]	196
Kapton-H (34)	75	"	250	1400
Kapton-H (34)	105	"	270	990
BPDA-DDBT (34)	95	"	2480	470
BPDA-DDBT (34)	105	"	1670	540
Kapton-H (37)	120	p/p_{sat} = 0.2 (pure H_2O)	80	NA
PEEK, T_p = 285°C	130	7.6 wt% H_2O in EtOH	371	~790
PEEK, T_p = 285°C	160	7.6 wt% H_2O in EtOH	374[c]	~88[c]

[a] 2.5 μm active layer of poly(vinyl alcohol) supported on poly(acrylonitrile).
[b] NA: Not available.
[c] p/p_{sat} for this mixture is 0.67.

at low water concentrations. Additionally, PEEK offers improved thermal, chemical, and mechanical stability, especially when it is rolltruded. PEEK, because of its overall stability, is also attractive for tackling more noxious separations, such as the vapor phase dehydration of acetic acid, as well as for higher temperature separations above 150°C for which many polymers prove to be unsuitable.

Rolltrusion membrane fabrication also offers several advantages over solution casting techniques, including

1. Ease of thin film production
2. Improved strength and creep resistance
3. The avoidance of noxious solvents otherwise needed for film casting

Item 3 also reduces health and safety concerns and eliminates the cost of solvent recovery. Elsewhere, it has been demonstrated that rolltrusion processing can be used to craze polymers in order to improve penetrant permeability in a polymer without sacrificing selectivity (10, 11). These advantages indicate that rolltruded polymers in general, and PEEK in particular, may be of practical value for membrane applications where harsh chemical environments are encountered.

CONCLUSIONS

In this paper rolltrusion processing has been employed in the fabrication of thin films of PEEK for membrane applications. Variations in the transport properties are found to be consistent with trends already noted by us, for example in rolltruded iPP films.

The combination of the excellent solvent resistance, improved mechanical properties, and good permeability and selectivity to water and ethanol vapor at temperatures well above 100°C suggests that rolltruded PEEK may be useful for membrane applications in harsh thermal and/or chemical environments for which commercially available polymeric membranes are simply inadequate.

ACKNOWLEDGMENT

The authors thank Dr. Mark Sefton of Imperial Chemical Industries, Wilton Works, UK, for the samples of PEEK used in this experimental work.

REFERENCES

1. R. Rautenbach and H. E. Ehresmann, *AIChE Symp. Ser. 272*, *85*, 48 (1989).
2. R. W. Dyson (Ed.), *Engineering Polymers*, Chapman and Hall, New York, NY, 1990.

3. C. Chau and R. A. Wessling, US Patent 4,957,817.
4. J. Koo, C. Chau, J. R. Racchini, R. A. Wessling, and M. T. Bishop, US Patent 4,992,485.
5. H. N. Beck, *J. Appl. Polym. Sci.*, *45*, 1361–1366 (1992).
6. D. C. Sun, E. M. Berg, and J. H. Magill, *Polym. Eng. Sci.*, *29*, 715 (1989).
7. M. J. Shankernarayanan, D. C. Sun, M. Kojima, and J. H. Magill, *Int. Polym. Proc.*, *1*, 66–76 (1987).
8. R. J. Ciora and J. H. Magill, *J. Polym. Sci., Polym. Phys. Ed.*, *30*, 1035–1044 (1992).
9. R. J. Ciora and J. H. Magill, *Ibid.*, *32*, 305–312 (1994).
10. R. J. Ciora and J. H. Magill, *J. Appl. Polym. Sci.*, *58*, 1021 (1995).
11. R. J. Ciora and J. H. Magill, *Polymer*, *35*, 949–955 (1994).
12. A. Peterlin, J. L. Williams, and V. Stannett, *J. Polym. Sci., Part A-2*, *5*, 957–972 (1967).
13. J. L. Williams and A. Peterlin, *Ibid.*, *9*, 1483–1494 (1971).
14. C. L. Choy, W. P. Leung, and T. L. Ma, *J. Polym. Sci., Polym. Phys. Ed.*, *22*, 707–719 (1984).
15. V. Vittoria, F. DeCandia, V. Capodanno, and A. Peterlin, *Ibid.*, *24*, 1009–1019 (1986).
16. M. A. Grayson and C. J. Wolf, *Ibid.*, *25*, 31–41 (1987).
17. C. J. Wolf, J. A. Bornmann, and M. A. Grayson, *Ibid.*, *29*, 1533–1539 (1991).
18. C. J. Wolf, J. A. Bornmann, and M. A. Grayson, *Ibid.*, *30*, 113–126 (1992).
19. M. A. Grayson and C. J. Wolf, *Ibid.*, *26*, 2145–2167 (1988).
20. J. N. Hay and D. J. Kemmish, *Polymer*, *29*, 613–619 (1988).
21. E. J. Stober and J. C. Seferis, *Polym. Eng. Sci.*, *28*, 634–639 (1988).
22. P. S. Pao, M. A. Grayson, and C. J. Wolf, *J. Appl. Sci.*, *35*, 726–732 (1988).
23. A. Peterlin, *Colloid Polym. Sci.*, *263*, 35–41 (1985).
24. H. L. Frisch and S. A. Stern, *CRC Crit. Rev. Solid State Mater. Sci.*, *20*, 65 (1980).
25. R. J. Pace and A. Datyner, *J. Polym. Sci., Polym. Phys. Ed.*, *17*, 453–464 (1979).
26. R. J. Pace and A. Datyner, *Ibid.*, *18*, 1169–1173 (1980).
27. D. J. Blundell and B. N. Osborn, *Polymer*, *24*, 953–958 (1983).
28. K. Friedrich, "Crazes and Shear Bands in Semi-Crystalline Thermoplastics," in *Advances in Polymer Science 52/53*, Springer-Verlag, Berlin, 1983, pp. 225–274.
29. T. Kataoka, T. Tsuru, S. Nakao, and S. Kimura, *J. Chem. Eng. Jpn.*, *24*, 334–339 (1991).
30. N. L. Thomas and A. H. Windle, *Polymer*, *23*, 529–542 (1982).
31. T. G Fox, *Bull. Am. Phys. Soc.*, *123* (1956).
32. R. F. Fedors, *J. Polym. Sci., Polym. Lett. Ed.*, *17*, 719–722 (1979).
33. R. B. Bird, W. E. Stewart, and E. N. Lightfoot, *Transport Phenomenon*, Wiley, New York, NY, 1960.
34. K. Okamoto, N. Tanihara, H. Watanabe, K. Tanaka, H. Kita, A. Nakamura, Y. Kusuki, and K. Nakagawa, *J. Membr. Sci.*, *68*, 53–63 (1992).
35. R. Rautenbach and U. Meyer-Blumenroth, *Desalination*, *77*, 295–322 (1990).
36. R. Rautenbach and R. Albrecht, *Membrane Processes*, Wiley, New York, NY, 1989.
37. S. I. Semenova, H. Ohya, T. Higashijima, and Y. Negishi, *J. Membr. Sci.*, *67*, 29–37 (1992).
38. U. Sander and H. Janssen, *Ibid.*, *61*, 113–129 (1991).
39. A. E. Jansen, W. F. Versteeg, B. van Engelenburg, J. H. Hanemaaijer, and B. Ph. ter Meulen, *Ibid.*, *68*, 229–239 (1992).

Received by editor March 9, 1996
Revision received May 14, 1996